Journal of Cardiovascular Translational Research (2022) 15:1119–1128
https://doi.org/10.1007/s12265-022-10229-w

METHODS PAPER

Customizable Angioplasty Balloon-Forming Machine: Towards Precision Medicine in Coronary Bifurcation Lesion Interventions

Kaitlyn M. Elmer[1] · Maxwell J. Bean[1] · Barry F. Uretsky[2] · Sam E. Stephens[1] · Hanna K. Jensen[3] · Morten O. Jensen[1]

Received: 11 June 2021 / Accepted: 25 February 2022 / Published online: 21 March 2022

Abstract

The ability to customize the size and shape of angioplasty balloons may be useful in many clinical and research applications of coronary and endovascular intervention. Fully customizable balloons are outside the reach of most researchers due to their prohibitive cost. A small-scale balloon-forming machine was developed to produce fully customizable balloons. This study describes the creation of this customizable balloon-forming machine and identifies the key components of manufacturing a patient-specific balloon. Using a standard balloon-shaped mold created with a novel application of 3D stereolithography-printed resin, 104 PET balloon formation tests were conducted. A statistical study was conducted in which molding temperature and inflation air pressure were independent variables ranging from 100 to 130 °C and from 3.7 to 6.8 atm, respectively. The criteria for balloon-forming success were defined; pressure and temperature combined were found to have a significant impact on the success ($p = 0.011$), with 120 °C and 4.76 atm resulting in the highest chance for success based on a regression model.

Keywords Balloon-forming machine · Stereolithography · Thermoplastic · Coronary intervention · Endovascular intervention · Balloon angioplasty · Coronary artery disease · Bifurcation lesion

Abbreviations

CAD	Coronary artery disease
BFM	Balloon-forming machine
PET	Polyethylene terephthalate

Introduction

Obstructive coronary artery disease (CAD), a common manifestation of heart disease, is characterized by the narrowing of the vessel lumen, limiting blood supply to heart tissue. Treatment of CAD often uses balloon inflation to first widen the narrowed lumen of an atherosclerotic lesion followed by implantation of a metallic stent to maintain the desired lumen diameter. CAD may occur in a variety of locations and complexities, with one particularly common (15–20% of coronary stenoses) and challenging lesion being at vessel bifurcations [1–7]. There are several techniques described to treat bifurcation lesions, but all have limitations. These techniques include so-called provisional stenting where the side branch is not stented, and bifurcation stenting, which includes "T-stenting," "culotte" stenting, "Y stenting," "crush, reverse crush mini-crush and DK crush," and "T in protrusion (TAP)" [1, 6–10]. These techniques either create overlapping stents or expose a location without stent coverage in the bifurcation; both conditions increasing the risk of restenosis. Also, during stenting of the main branch in a bifurcation lesion, the side branch is susceptible to occlusion. The jailed wire technique places a wire in the side branch during stenting of the main branch, maintaining access to the side branch should occlusion occur; however, the jailed wire technique also adds increased risk for fracture of the jailed wire during removal [1, 11]. Additional complications may arise as each bifurcation is different in geometry, vessel size, and separation angle [12–14]. Furthermore, the level of

Associate Editor Adrian Chester oversaw the review of this article .

✉ Morten O. Jensen
mojensen@uark.edu

[1] Department of Biomedical Engineering, University of Arkansas, Fayetteville, AR, USA

[2] Department of Internal Medicine, University of Arkansas for Medical Sciences, Little Rock, AR, USA

[3] Departments of Surgery and Radiology, University of Arkansas for Medical Sciences, Little Rock, AR, USA

calcification present in lesions also influences treatment strategies [15, 16].

Whether used in conjunction with stents or alone, current methodologies normally use various sizes of cylindrically shaped angioplasty balloons to treat both straight and bifurcation lesions [3, 7, 17–24], though some specific bifurcation-shaped balloon-stent systems exist historically and are currently commercially available [25–27]. For example, bifurcation-specific balloon-stent systems have used bottle-shaped balloons to better accommodate changing diameters along vessel length [26]. Customized balloons have the potential to improve patient outcomes; for example, bifurcation-shaped balloons may help reduce malapposition of stents and improve expansion at the bifurcation on vessel walls. However, commercially available balloons for bifurcation treatment are currently cylindrical in shape and come in a standardized set of sizes. Specific and customized balloon shapes to treat the bifurcations do not exist. Due to factors such as lead time and overall creation cost, any custom balloon shapes and sizes are not available in a rapid and cost-effective manner. Therefore, there is a need for readily available customizable balloons for the study of various bifurcation-shaped balloons to evaluate potential solutions.

In this study, a balloon-forming machine (BFM) was developed for the purpose of producing balloons with customizable size and shape for a variety of CAD lesions. The methods described here create balloons suited for laboratory studies, though with additional development and modification, the BFM could be used clinically as well. The BFM described produces balloons for lower costs and quicker lead times than those currently available, albeit in much lower production volume than commercial BFMs. Angioplasty balloons are generally created using blow molding, a process that uses air pressure and heat to inflate a parison into the desired shape [28–31]. "Parison" is an industry term for the sealed thermoplastic tube that becomes the balloon upon inflation. The BFM described in this study follows this general methodology, utilizing molds created with additive manufacturing of a high-temperature resin. This mold design allows for quick and cost-effective customizability.

To optimize the design and use of the BFM, parameters that contribute to balloon-creation success while using a customizable mold were identified. BFMs are typically industrially controlled systems, with operating parameters and protocols tightly controlled and tailored to specific balloon geometries. By bracketing some of these important parameters onto a low-volume BFM, the accessibility and utility of such a machine may be increased. This innovation enables better design and testing with regard to novel balloon-stent techniques.

Methods

Balloon sizes and materials were selected based upon two major parameters: availability and manufacturing complexity. Balloons in this study were designed from polyethylene terephthalate (PET), a common industry balloon material, with parison dimensions of 3.35 mm OD (0.132 in), 2.54 mm ID (0.1 in), and approximately 120 mm in length. The goal was to create a balloon of 16 mm OD and 45 mm in length. These dimensions, which will yield balloons larger than those clinically used for coronary angioplasty and stenting, were selected to improve handling of the devices and inspect initial parameter dependency on the outcomes. However, the process described here can be scaled down to create smaller balloons to fit coronary and peripheral vessels.

Balloon-Forming Machine Design

Briefly, angioplasty balloons are generally created by heating a sealed, thermoplastic tube connected to a pressurized air source inside of a balloon-forming machine [28–31]. Through a combination of heat and pressurized air, the tube, referred to in industry as a parison, is inflated to fill a mold cavity and achieve a desired size and shape with minimal wall thickness to insure consistent deployment properties, as well as creating a thin profile to allow the crimped balloon to enter a constricted blood vessels [28–31].

All balloons in this comparative study were created using the custom BFM described below, inspired by previously published schematics of industrial BFMs [32, 33].

Figure 1 shows the basic elements of the custom BFM. Figure 1D shows the 50 mm × 50 mm × 100 mm aluminum block that houses the mold and the four 2.5 in (63.5 mm) cartridge heaters. The mold was created using a stereolithography additive manufacturing resin (HIGH TEMP Photopolymer Resin FLHTAM02, Formlabs, Somerville, MA) along with two stopper ends that are inserted into each end of the mold during balloon formation. The stopper ends shape the balloon ends and prevent excessive axial movement during inflation. The resin mold replaces the traditional "glassform" used to hold the shape for the expanding plastic to push against and create the desired balloon shape and size [32, 33]. A high-temperature stereolithography resin was used rather than a blown glass form because the resin is considerably less expensive to produce as compared to blown glass. Using additive manufacturing also allowed for simple and quick prototype changes while mimicking more expensive glass' maximum temperature withstanding and heat conduction capabilities. The mold

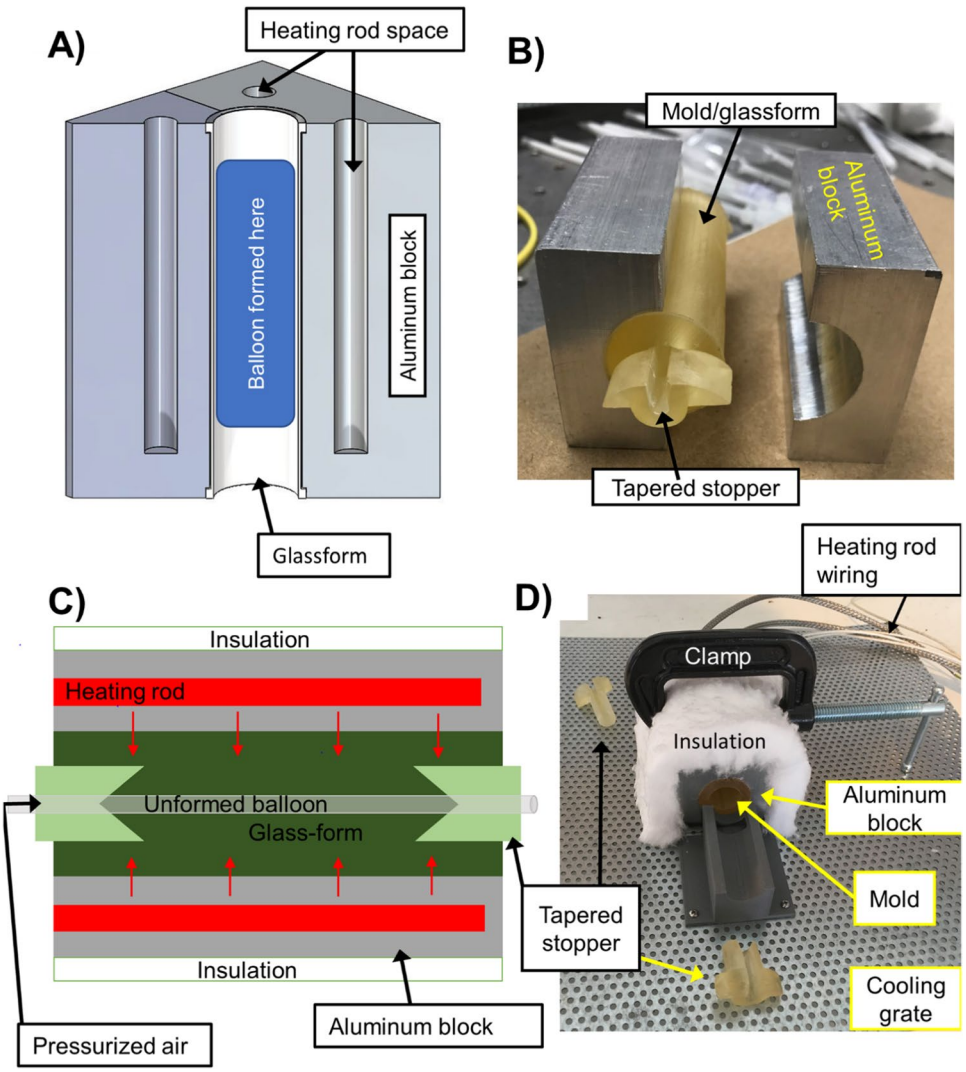

Fig. 1 Custom balloon-forming machine: A 3-Dimensional rendering of interior design. Balloons are formed inside mold as indicated. B Photo of the interior of the system. C 2-Dimensional diagram of the system outlined in A and B; heating rods provide evenly distributed heat (red arrows) to pressurized tubes of unformed balloons. When optimal temperature and heat time are reached, pressure is increased and balloon is formed. D Photo of the BFM

was encapsulated by two halves of the above mentioned aluminum block on top of a grate to allow even air flow on all sides of the device. The block hosted four 250-W heating rods, with one rod also incorporating a thermocouple for temperature measurements. The temperature measurement was only necessary in one rod since the setup is symmetric. The heating rods were attached to a proportional-integral-derivative (PID) heater controller (Model TA4, Mypin Electrical Co., Zhongshan, Guangdong, China) to maintain proper temperature during operation. The maximum observed overshoot was 10 °C after using the MyPin's autotune feature to set PID values. The temperature was allowed to settle before balloon forming. A layer of carbon fiber insulation covers the main component of the machine in Fig. 1D to reduce temperature variations induced by convective air currents in ambient air.

A multi-component design was used for the mold to accommodate the number of balloons planned for this study. Instead of creating a mold that would have the complete contour of the balloon, including the tapers at the ends, this design used a cylindrical mold with two removable stoppers, shown in Fig. 1. The stoppers form the desired tapered geometry at the balloon ends. Because they are removable, the balloon and stoppers can be quickly removed and cooled following balloon creation instead of requiring cooling and disassembly of the entire BFM. These removable ends were tapered at an angle of 30° and 22 mm long.

Balloon Creation Process

Balloons were created from off-the-shelf PET tubing of 0.132″ OD and 0.1″ ID (1000160PET05, Nordson Medical, Westlake, OH). These tubes were created by using cyanoacrylate glue to seal one end of the tube and attaching the other end to a Luer lock attachment for connection to a compressed air source (AirMate AM78-HC4V, Emglo,

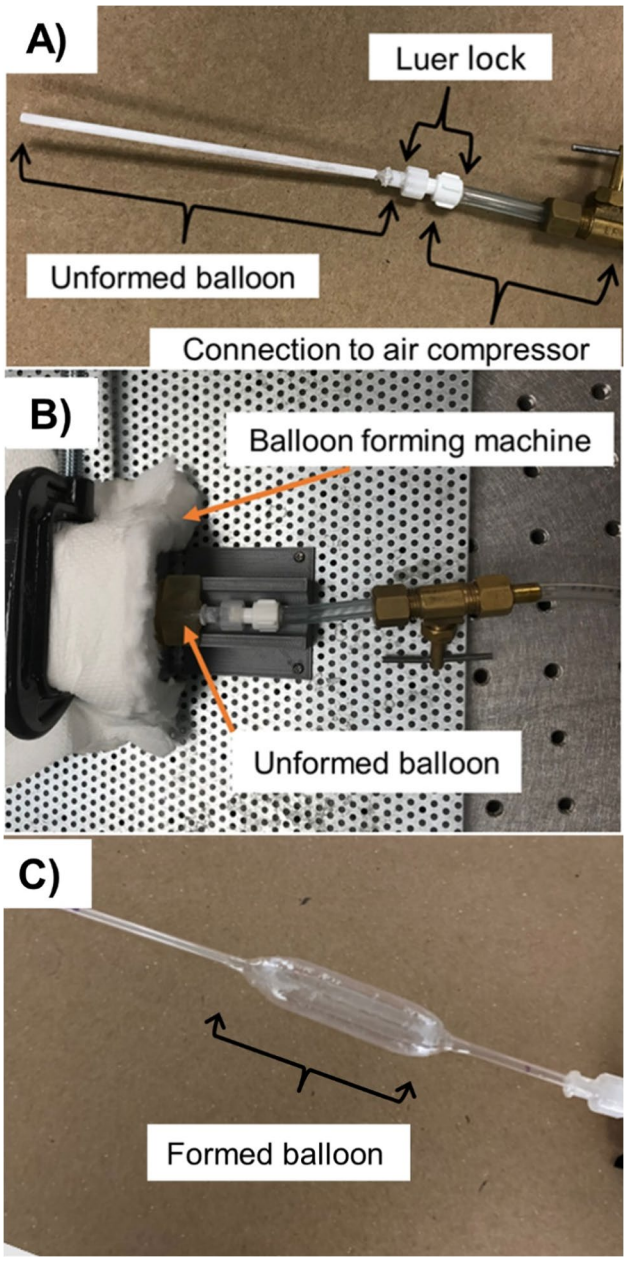

Fig. 2 Process of balloon creation. A Unformed balloon attached to air compressor via Luer lock. B Balloon parison heating in BFM. C Balloon after removal from BFM, still attached to the air compressor

Somerset, PA), as seen in Fig. 2A. These prepared tubes were modeled after industrial parisons.

The BFM was preheated to the desired temperature, and the regulator of the air compressor was set to the desired inflation pressure. Temperatures were verified using a probe thermometer touching the inside wall of the mold (Traceable Kangaroo 1230N27, Thomas Scientific, Swedesboro, NJ). Once the desired temperature was confirmed with the probe thermometer, the prepared tube was attached to an air compressor using a Luer lock, as seen in Fig. 2A. The two stoppers were inserted into both ends of the mold. The connected parison was inserted into the mold for the desired heating time, seen in Fig. 2B. Once the heat time was completed, the air valve was opened, allowing the balloon to be formed. The valve was kept open until the balloon was created or a failure was detected; the valve was usually open for 1–3 s. Then, the newly formed balloon was removed from the mold and cooled to room temperature, as seen in Fig. 2C. If the balloon did not deploy or burst at the designated time when pressurized, the parison was air cooled and the process restarted.

Determining Significant Balloon Forming Parameters

In the use of the BFM, four independent parameters appeared to affect the creation of the balloon: mold temperature, inflation pressure, heat time, and mold design [28, 34]. An experiment was conducted with 104 sample balloons created at four separate temperatures, 100 °C, 110 °C, 120 °C, and 130 °C. These temperatures are 20–40 °C higher than the glass transition temperature of PET plastic (87 °C), the typical range used in industry [35]. The pressure was varied between 4.1 and 7.8 atm (60–115 psi) in intervals of 0.34 atm (5 psi). After preliminary testing, the heat time was kept constant at 30 s. A standard-shaped balloon, consisting of a constant diameter and identical tapers at both ends of the balloon, was chosen to keep a constant profile with a diameter of 16 mm and a length of 53 mm. These values were chosen based on industry balloons of the same size and shape (10004013 EB, Nordson Medical, Westlake, OH), which are about twice the diameter of the largest stent carrying balloons marketed for coronary arteries (H7493942808350, Boston Scientific, Marlborough, MA). The double wall thickness, which is single wall thickness times two, is measured by the thickness of the balloon when deflated across both walls and is tightly correlated to the maximum pressure that a balloon can reach. For the balloons created, the desired double wall thickness is 2–2.4 mils (0.05–0.06 mm). This parameter was determined from comparison to industry standards and by deriving Barlow's formula to determine the ultimate burst pressure:

$$P_t = 2 * S_t * \frac{t}{d_0}$$

where P_t is the ultimate burst pressure, S_t is the ultimate tensile strength, t is the thickness of the balloon wall, and d_0 is the diameter of the balloon [36]. To avoid balloon rupture during a procedure, the thickness needs to be sufficient to

safely withstand around 12 atm of inflation pressure while maintaining a thin profile for traversing tight lesions [31].

Successful Balloon Criteria

A slight "bow" in the shape of the balloon during the cooling phase was evident at some instances by using this technique. This bowing seemed to originate from the manual aspects of the balloon forming process (see below) and the effect of gravity on the balloon while still hot. For example, removing the newly formed balloon from the mold by hand can cause some deformation in the still malleable balloon structure. The user error component was rectified with a procedure update to allow for the balloon to be cooled facing downwards, with the circular cross section of the balloon parallel to the floor, to reduce the effect of gravity. In addition, a metric named "skew ratio" was created, the formula for which is shown below:

$$\text{Skew ratio} = \frac{d_{\text{skew}} - d_{\text{avg.}}}{d_{\text{avg.}}} \times 100\%$$

The skew diameter, d_{skew}, is measured by laying the balloon down on a flat surface to clearly reveal any bowed effect. An image was taken, and two parallel lines were superimposed and used to measure the shortest length between the top and bottom of the balloon. If the balloon was bowed, the measured skew diameter would be higher than the average diameter, and if less bowed, the skew diameter and average diameter would be similar. An example of measuring the skew diameter is shown in Fig. 3F. The average diameter, d_{avg}, was measured across three diameters, one taken on each end and the third in the approximate center.

Balloons were classified under a variety of criteria. Balloon creation was considered successful if they: (1) did not have any visible punctate balloon defects, (2) the

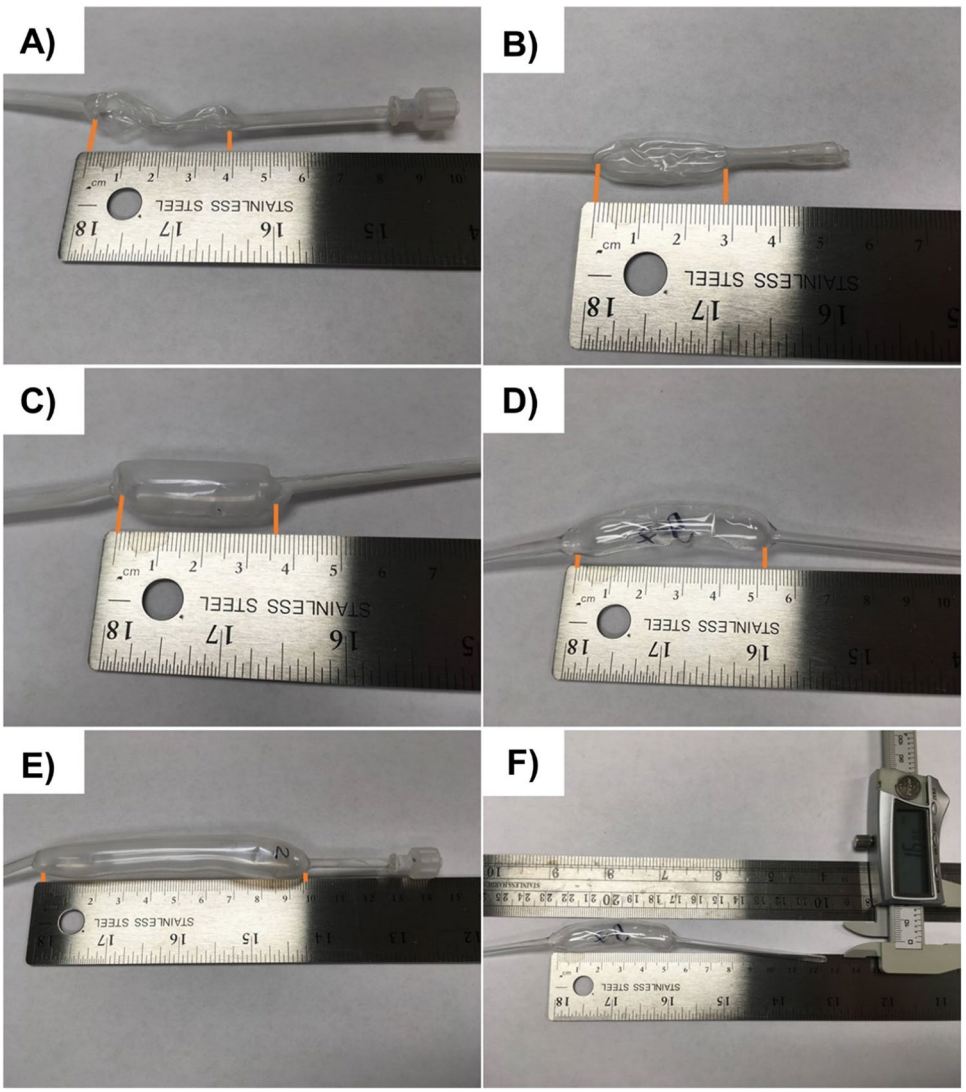

Fig. 3 Examples of results from balloon deployments. Criteria of balloon failure modes and success are illustrated: A burst balloon, B small diameter, C short length, D failed-high skew ratio, E success F demonstrating the method of measuring the skew diameter

average balloon diameter was within 20% of the intended result (16 mm), (3) the skew ratio was less than 0.125, and (4) the length was greater than 45 mm. Each balloon was visually inspected for any holes, had its diameter measured in three locations, and had its length and skew diameter measured. The length was measured along the cylindrical length of the balloon within the tapered ends. Figure 3 shows where the length was measured, with orange lines indicating starting and stopping points just inside the two tapered regions. If any of the criteria were not met, the balloon was not considered acceptable. For prototyping purposes, the acceptable measurements were widened so that a balloon with a diameter up to 20% smaller than intended, a slight skew ratio of 0.125 or less, and at least the length of stent models used (45 mm) was considered acceptable.

Figure 3 shows the examples of the different common failure methods as well as a comparison to a success. Figure 3A shows a punctured balloon, in this case from a high temperature and pressure combination. Figure 3B shows a balloon with insufficient length and diameter. Figure 3C shows a balloon that is too short, being 36 mm when at least 45 mm is acceptable. Figure 3D shows a balloon with a skew ratio that is too large. Figure 3E shows a balloon that is considered a success. Figure 3F shows how the skew diameter was measured.

Statistical Tests

A nominal logical fit for success using a chi-squared test was applied to the results from the balloon study. The equation below represents the model used in the analysis:

$$Y = \frac{1}{1 - e^{-(\beta_0+\beta_1 X_1+\beta_2 X_2+\beta_3 X_1 X_2+\in)}}$$

where:

- Y is the probability of success
- X_1 is the wall temperature on the BFM
- X_2 is the inflation pressure
- β_0 represents the intercept for the model
- β_1 represents the constant for the wall temperature
- β_2 represents the constant for the air pressure
- β_3 represents the constant for the combination of pressure and temperature
- $\in$ is the independent error term that follows a normal distribution with mean 0 and equal variance σ^2

Our null hypothesis is as follows:

$$H_0 : \beta_1 = \beta_2 = \beta_3 = 0$$

$$H_A : \text{At least one } \beta_j \neq 0$$

This test determines whether there are one or more significant parameters affecting balloon-forming success and which parameters (temperature and/or pressure) are the most likely to significantly impact the likelihood of success. A p-value of 0.05 or lower was considered significant. All analyses were run using JMP (SAS Institute, Cary, NC).

A statistical analysis using the likelihood ratio chi-squared statistic ($G^2 = 2\sum_i \sum_j n_{ij} \ln(\frac{n_{ij}}{e_{ij}})$), which is based on the ratio of the observed to the expected frequencies, was also calculated.

Results

The statistical analysis using the likelihood-ratio chi-squared is demonstrated in Table 1. These results suggest that pressure and temperature combined have a statistically significant influence on the success of the balloon creation process, χ^2, $(1, N = 104) = 9.92$, $p = 0.008$. Table 2 shows the mean measurement values for successful balloons in each temperature group and for all groups combined. Figure 4 shows the graphical representation of the regression model fitted to the data and employed in the statistical test. A higher likelihood of success can be seen within a low temperature and low-pressure range and a high temperature and high-pressure range.

Using the equation for volume of a tube, if the tubes were to expand exactly to the desired diameter, without any axial stretch, the double wall thickness should be thicker than what was found experimentally. The equation below is derived from the volume of a tube:

$$V_{\text{tube}} = V_{\text{balloon}}$$
$$L_1 \frac{\pi}{4}\left((D_{1o})^2 - (D_{1i})^2\right) = L_2 \frac{\pi}{4}\left((D_{2o})^2 - (D_{2i})^2\right)$$

Subscript "2" is before the balloon formation, and "1" is after. Subscripts o and i denote the outer and inner diameter, respectively. For example, L_2 is the length of the tube before

Table 1 Statistical results from the likelihood ratio chi-squared statistic (G^2) which is based on the ratio of observed-to-expected frequencies of balloon creation success. Pressure is shown to be significant ($P < 0.05$). The temperature and pressure combination is also significant with a stronger P-value ($P < 0.01$)

Statistical significance of parameters on balloon creation success		
Source	G^2	P-value
Temperature	0.479	0.489
Pressure	4.545	0.033*
Temperature and pressure	7.096	0.008*

Table 2 Mean and standard deviations of properties for successful balloons at different temperature groups and for all groups combined

Temp	Pressure (atm)		Diameter (mm)		Skew ratio		Length (mm)	
	Mean	SD	Mean	SD	Mean	SD	Mean	SD
100 °C	5.1	0.28	13.9	0.78	1.06	0.037	62.7	16.6
110 °C	5.2	0.43	13.8	0.79	1.16	0.023	67.6	13.4
120 °C	4.7	0.37	13.5	0.44	1.12	0.020	54.4	10.9
130 °C	4.8	0.15	13.9	0.48	1.11	0.029	53.4	9.1
Combined temp	4.9	0.49	13.6	0.61	1.11	0.053	56.6	12.3

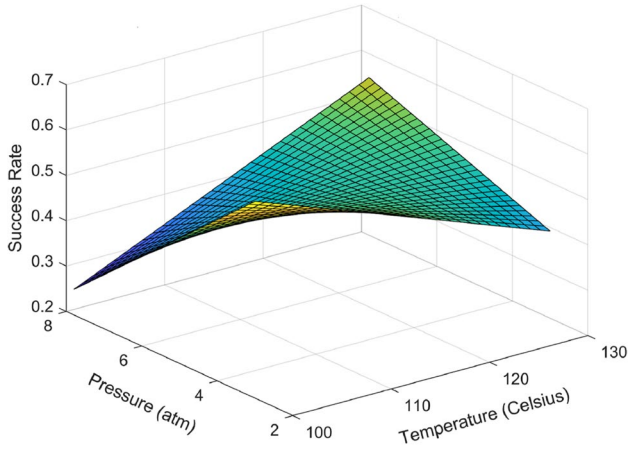

Fig. 4 A graphical representation of the probability of success as depending on the relationship between temperature and pressure. The equation for the probability of success is $z = 0.004 \times y - 0.019\ x - 0.449\ y + 2.785$ where x is the temperature, y is the pressure, and z is the probability of success

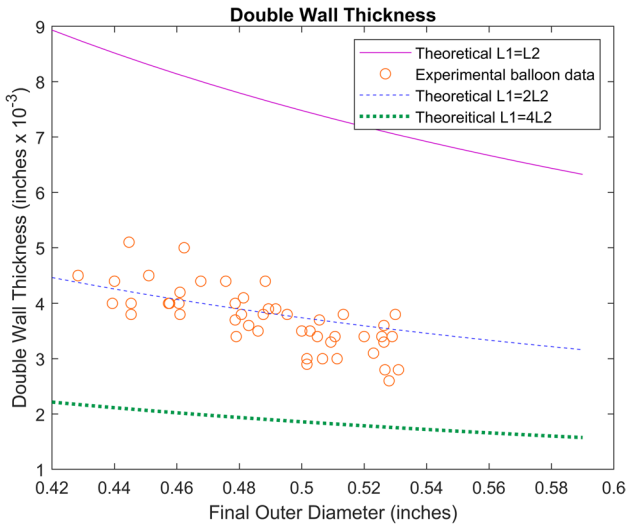

Fig. 5 Theoretical and experimental double wall thickness with respect to the final outer diameter. Double wall thickness is the measured thickness of the deflated balloon. L_2 is the length of the balloon material before balloon forming and L_1 is the length after balloon forming. Three lines at different $\frac{L_1}{L_2}$ values are shown, as well as experimental data. Assuming the balloon expands only radially, gathered data should lie around the solid line. However, the data lies around a $\frac{L_1}{L_2} = 2$ ratio meaning that the balloon expands to twice the original length

balloon forming and D_{1i} is the inner diameter of the balloon after forming.

Inserting $D_i = D_o - t_d$ for D_{2i}, the solution for t_d (double wall thickness of the balloon) can be found:

$$t_d = D_{1o} - \sqrt{D_{1o}^2 - \frac{L_2}{L_1}\left(D_{2o}^2 - D_{2i}^2\right)}$$

Figure 5 is a representation of the equations discussed above. This graph compares theoretical double wall thicknesses with what was experimentally measured. The solid purple line indicates the projected double wall thickness if $L_1 = L_2$. This would be true if there was no stretch axially when the balloon is created. The experimental data is shown with the orange circles. The dashed blue line indicates the ratio of $L_1 = 2\ L_2$ from the same equation, corresponding to the data gathered. The dotted green line indicates the industry standard double wall thickness values to reduce the balloon profile to a minimum amount while still being considered strong enough to withstand the pressure requirements [35].

Discussion

There are numerous parameters in a complex interaction that contribute to the proper creation and molding of plastics [34]. As such, the balance between temperature and pressure is necessary to carefully consider. It was found that within the presented BFM's tested range of 3.7 to 7.8 atm (55–115 psi) and 100–130 °C, a combination of pressure and temperature has the largest impact on the outcome of the balloon. Pressure alone was also statistically significant, while temperature alone was not identified as a significant variable. This seems to be because successful balloons were created at each temperature, but

successful balloons were created within a smaller band than the tested range of pressures. Pressures from 4.1 to 5.8 atm (60–85 psi) were used to create acceptable balloons, with the mean across all groups being 4.9 atm. One standard deviation from the mean gives pressures from 4.41 to 5.39 atm. The model predicts that 4.75 atm and 112.25 °C will have the highest chance of success, with 4.75 atm being well within one standard deviation from the mean in the success group. This indicates a consistent range of values for balloon creation success. Clearly, a careful balance of both temperature and pressure is needed for optimal performance of the BFM. As shown in Fig. 5, a higher likelihood of success can come from a steady increase of both heat and pressure.

Another important observation made is displayed in Fig. 5. Knowing that the plastic will naturally expand radially is useful in any balloon-forming design. It can be theorized that balloon double wall thickness can be controlled by pulling the balloon axially during formation. This is used in many commercial balloon-forming machines [28, 37, 38]. An apparatus that pulls axially on the balloons during formation is one potential improvement that can be made to the BFM. Since some existing methodologies use automated technology, an automated system to stretch the balloons may be beneficial as well [28, 32]. Future tests are required to determine the effectiveness of stretching the balloon to create uniformly thin-walled balloons.

Further work in eliminating variability in balloon forming is in progress. Due to the manual nature of operating air supply valves, the parison tends to move, contributing to uneven parisons heating and balloon deformations. Stabilizing the air hose with a stand/clamp reduces the motion of the air hose and parison. The stoppers also tend to move during pressurization, which contributes to variations in balloon length. Small quick-release clamps aid with keeping the stopper ends secure and allow for easy removal after balloon formation. Another way to remove variability is by easing operator use of the BFM. Balloons created in this study can be difficult to remove from the BFM while fully inflated. A second valve connecting the air hose to the atmosphere can be opened slightly after balloon formation, which relieves some of the pressure in the balloon. Then, after removing the balloon from the BFM, the valve to the air supply can be partially opened to completely reinflate the balloon during cooling. This measure appears to help the balloon maintain the desired shape during cooling, though the manual nature requires some operator skill to remove and reinflate quickly before the balloon cools.

Due to the balloons in this study being cooled with the circular cross-section parallel to the ground, the balloon material has the potential to move downwards during cooling, contributing to uneven wall thicknesses. Using a device to rotate the balloons during cooling may keep material from being unevenly distributed along the length of the balloon. Also, using a fan or other cooling mechanism may cool the balloons quicker than ambient air, locking in the desired balloon shape. Further work is required to determine the best method for cooling balloons.

The main advantage of the current design is the ability to create balloons of varying geometry quickly and cost-effectively. By changing the 3D formable resin molds, custom balloons can be specifically shaped and tested. Bifurcation lesions are a large motivation for the creation of this device, though treatment of straight lesions may also be improved with custom balloon geometries. To customize to a bifurcation shape, the geometry may be designed with "generic" features (for example, a generalized tapered shape) or be derived from specific patient data (for example, patient CT scans) [39]. As the mold can be created in less than 24 h, virtually, any design can be rapidly created and iterated for research applications. The cost of the 3D printed resin molds is about $1.00/mold (RS-F2-HTAM-02, Formlabs, Somerville, MS), and coupled with the cost of parison materials being about $2.00/parison (51525K425, McMaster-Carr, Elmhurst, Il; 1000160PET05, Nordson Medical, Westlake, OH); the balloons created by the BFM are significantly less expensive than customizable balloons found on the market, which starts at about $18.00 each (10004017EA, Nordson Medical, Westlake, OH) for a semi-custom balloon. Fully customizable balloons are much higher in cost, requiring custom-made parts such as glassforms. The time and cost efficiency of creating a wider range of balloon geometries with the BFM will aid in the treatment of a wide variety of lesions in CAD by easing the process of optimizing balloon geometry. Scaling the BFM to sizes used in percutaneous and coronary arteries will also be enabled by the ease of resin mold creation. For scaling the machine, the principle components will remain similar, with optimization for the potential variations in heat transfer associated with a smaller mold and parison. The pressure required for smaller diameter parisons is expected to be larger based on Laplace's law. In addition, a shorter heat time is anticipated from the smaller volume of material in a smaller parison, and the temperature range is expected to see little to no change as the material properties of the parison will remain the same. Preliminary work in our laboratory appears to agree with these anticipated changes, and while that is beyond the scope of this current report, this will be the subject of future publications from this project.

The balloons created in this study differ from industrially created balloons in specific areas. Firstly, the balloons are connected to the inflation medium via Luer lock, rather than, for example, being attached to a dual-lumen catheter via specialized heat shrink tubing [40]. In the preliminary work, balloons created with the BFM have been attached to two separate lumens, one for a guidewire and one for

inflation, using cyanoacrylate glue. This allows for conducting tests in the laboratory within human tissue-mimicking gel phantoms [41]. Second, as previously alluded to, industrially created balloons undergo axial stretching processes [28, 35, 42]. These processes can vary, but the key reasons they are used are to create thinner wall balloon wall thickness and to biaxially orient the balloon material. Finally, the current BFM has a low rate of acceptable balloon creation, which is expected for a prototype system. In contrast, industrial processes are automated, allowing higher levels of repeatability and tighter tolerances in balloons. For these reasons, the current process is initially most useful for laboratory applications, though with further development of the described BFM, these differences will be resolved and the device will be cost-effective enough to be available for clinical use. However, plaques in CAD have a spectrum of properties, and an ability to create and easily test various balloon geometries in clinically relevant proportions has the potential to aid physicians in customizing patient-specific treatment for straight or bifurcation lesions.

Conclusion

In summary, the purposes of this study were to describe a customizable BFM, to establish general parameters for using the described device, and to highlight practical solutions for improving the functionality of the machine. To this end, a custom BFM was created and a relationship between parameters was found for creating balloons with desirable properties. This system, using a mold created from additive manufacturing, was able to properly function in creating usable angioplasty style balloons. High temperatures, around 20–40 °C higher than the glass transition temperature of PET (87 °C), were found to be an optimal range for balloon creation but only with pressures ranging from 4.8 to 5.4 atm. These two parameters combined resulted in creating balloons with desired properties in the machine model shown. This process demonstrates the possibility of smaller custom BFMs for labs to incorporate and modify depending on their intended design.

Acknowledgements Special acknowledgement to the American Heart Association in supporting the funding for this research.

Funding This study was funded by the American Heart Association grant # 18AIREA33960590.

Declarations

Ethics Approval This article does not contain any studies with human participants or animals performed by any of the authors.

Conflict of Interest The authors declare no competing interests.

References

1. Lassen, J., Burzotta, F., Banning, A., Lefèvre, T., Darremont, O., Hildick-Smith, D., et al. (2018). Percutaneous coronary intervention for the left main stem and other bifurcation lesions: 12th consensus document from the European Bifurcation Club. *EuroIntervention, 13*(13), https://doi.org/10.4244/EIJ-D-17-00622.
2. Rizik, D. (2010). Treating bifurcation coronary artery disease. *Reviews in Cardiovascular Medicine, 11*(1), https://doi.org/10.3909/ricm11S1S0006.
3. Park, T. K., Park, Y. H., Song, Y. B., Oh, J. H., Chun, W. J., Kang, G. H., et al. (2015). Long-term clinical outcomes of true and non-true bifurcation lesions according to Medina classification – Results from the COBIS (coronary bifurcation stent) II registry. *Circulation Journal, 79*(9), 1954–1962. https://doi.org/10.1253/circj.CJ-15-0264
4. Louvard, Y., Lefèvre, T., & Morice, M. (2004). Percutaneous coronary intervention for bifurcation coronary disease. *Heart,* 90, 713–722. https://doi.org/10.1136/hrt.2002.007682
5. Dash, D. (2014). Recent perspective on coronary artery bifurcation interventions. *Heart Asia, 6*(1), 18–25.
6. Louvard, Y., Thomas, M., Dzavik, V., Hildick-Smith, D., Galassi, A. R., Pan, M., et al. (2008). Classification of coronary artery bifurcation lesions and treatments: Time for a consensus! *Catheterization and Cardiovascular Interventions, 71*(2), 175–183. https://doi.org/10.1002/ccd.21314
7. Antoniadis, A. P., Mortier, P., Kassab, G., Dubini, G., Foin, N., Murasato, Y., et al. (2015). Biomechanical modeling to improve coronary artery bifurcation stenting: Expert review document on techniques and clinical implementation. *JACC: Cardiovascular Interventions, 8*(10), 1281–1296 https://doi.org/10.1016/j.jcin.2015.06.015.
8. Vorvick, L. J. (2019). Percutaneous transluminal coronary angioplasty (PTCA). Medline Plus. Retrieved 25 March, 2021, from https://medlineplus.gov/ency/anatomyvideos/000096.htm.
9. Singh, J., Depta, J., & Patel, Y. (2017). Bifurcation lesions. The Cardiology Advisor. Retrieved 25 March, 2021, from https://www.thecardiologyadvisor.com/home/decision-support-in-medicine/cardiology/bifurcation-lesions/.
10. Gwon, H. (2018). Understanding the coronary bifurcation stenting. *Korean Circulation Journal, 48*(6), 481–491. https://doi.org/10.4070/kcj.2018.0088
11. Hahn, J., Chun, W. J., Kim, J., Song, Y. B., Oh, J. H., Koo, B., et al. (2013). Predictors and outcomes of side branch occlusion after main vessel stenting in coronary bifurcation lesions: Results from the COBIS II registry (COronary BIfurcation Stenting). *Journal of the American College of Cardiology, 62*(18), 1654–1659. https://doi.org/10.1016/j.jacc.2013.07.041
12. Medrano-Gracia, P., Ormiston, J., Webster, M., Beier, S., Ellis, C., Wang, C., et al. (2017). A study of coronary bifurcation shape in a normal population. *Journal of Cardiovascular Translational Research, 10*(1), 82–90. https://doi.org/10.1007/s12265-016-9720-2
13. Ki, Y., Jung, J. H., Han, J., Hong, S., Cho, J. H., Gwon, H., et al. (2020). Clinical implications of bifurcation angles in left main bifurcation intervention using a two-stent technique. [Research Article]. *Journal of Interventional Cardiology, 2020*, https://doi.org/10.1155/2020/2475930.
14. Suleiman, S., Coughlan, J., Touma, G., & Szirt, R. (2021). Contemporary management of isolated ostial side branch disease: An evidence based approach to Medina 001 bifurcations. *Interventional Cardiology, 16*(e06), https://doi.org/10.15420/icr.2020.30.

15. Reifart, N., Vandormael, M., Krajcar, M., Göhring, S., Preusler, W., Schwarz, F., et al. (1997). Randomized comparison of angioplasty of complex coronary lesions at a single center: Excimer laser, rotational atherectomy, and balloon angioplasty comparison (ERBAC) study. *Circulation, 96*(1), 91–98. https://doi.org/10.1161/01.CIR.96.1.91
16. Noguchi, T., Miyazaki Md, S., Morii, I., Daikoku, S., Goto, Y., & Nonogi, H. (2000). Percutaneous transluminal coronary angioplasty of chronic total occlusions. Determinants of primary success and long-term clinical outcome. *Catheterization and Cardiovascular Interventions: Official Journal of the Society for Cardiac Angiography & Interventions, 49*(3), 258–264.
17. Steigen, T. K., Maeng, M., Wiseth, R., Erglis, A., Kumsars, I., Narbute, I., et al. (2006). Randomized study on simple versus complex stenting of coronary artery bifurcation lesions: The Nordic bifurcation study. *Circulation, 114*(18), 1955–1961. https://doi.org/10.1161/CIRCULATIONAHA.106.664920
18. Sgueglia, G. A., & Chevalier, B. (2012). Kissing balloon inflation in percutaneous coronary interventions. *JACC: Cardiovascular Interventions, 5*(8), 803–811, https://doi.org/10.1016/j.jcin.2012.06.005.
19. Elabbassi, W., & Al Nooryani, A. (2017). Skirt followed by trouser stenting technique: True anatomical preservation of coronary Y-shaped bifurcation lesions while using "vanishing" bioresorbable scaffolds: A report of two cases. *Cardiovascular Revascularization Medicine, 18*(4), 281–286. https://doi.org/10.1016/j.carrev.2016.10.007
20. Arokiaraj, M. C., De Santis, G., De Beule, M., & Palacios, I. F. (2016). A novel tram stent method in the treatment of coronary bifurcation lesions – Finite element study. *PLoS ONE, 11*(3), e0149838. https://doi.org/10.1371/journal.pone.0149838
21. Belardi, J. A., & Albertal, M. (2014). Self-Expanding dedicated bifurcation stent. *Catheterization and Cardiovascular Interventions, 84*(7), 1071–1072. https://doi.org/10.1002/ccd.25692
22. Chen, S., Sheiban, I., Xu, B., Jepson, N., Paiboon, C., Zhang, J., et al. (2014). Impact of the complexity of bifurcation lesions treated with drug-eluting stents. *JACC: Cardiovascular Interventions, 7*(11), 1266–1276 https://doi.org/10.1016/j.jcin.2014.04.026.
23. Colombo, A., & Ruparelia, N. (2015). When you ask yourself the question "should I protect the side branch?": The answer is "yes"∗. *JACC: Cardiovascular Interventions, 8*(1, Part A), 47–48 https://doi.org/10.1016/j.jcin.2014.11.007.
24. Yamashita, T., Nishida, T., Adamian, M. G., Briguori, C., Vaghetti, M., Corvaja, N., et al. (2000). Bifurcation lesions: Two stents versus one stent—Immediate and follow-up results. *Journal of the American College of Cardiology, 35*(5), 1145–1151. https://doi.org/10.1016/S0735-1097(00)00534-9
25. Ormiston, J., Webster, M., El-Jack, S., McNab, D., & Simpson Plaumann, S. (2007). The AST petal dedicated bifurcation stent: First-in-human experience. *Catheterization and Cardiovascular Interventions, 70*(3), 335–340. https://doi.org/10.1002/ccd.21206
26. Gil, R., Vassilev, D., & Bil, J. (2013). Dedicated bifurcation drug-eluting stent BiOSS - A novel device for coronary bifurcation treatment. *Interventional Cardiology Review, 8*(1), 19–22 https://doi.org/10.15420/icr.2013.8.1.19.
27. Morlacchi, S., Chiastra, C., Cutri, E., Zunino, P., Burzotta, F., Formaggia, L., et al. (2014). Stent deformation, physical stress, and drug elution obtained with provisional stenting, conventional culotte and Tryton-based culotte to treat bifurcations: A virtual simulation study. *EuroIntervention, 9*, 1441–1453. https://doi.org/10.4244/EIJV9I12A242
28. Patel, K. A., Patel, S. R., & Zimmerman, S. A. (1999). Method for making medical balloon catheter. In S. United (Ed.): Medtronic Inc.
29. Jhun, C., Rosenberg, G., & Waybill, P. (2015). Effect of angioplasty balloon compliance on stenotic blood vessel stress. *J Medical Devices, 9*(3), https://doi.org/10.1115/1.4030575.
30. Sauerteig, K., & Giese, M. (1998). The effect of extrusion and blow molding parameters on angioplasty balloon production. https://www.mddionline.com/news/effect-extrusion-and-blow-molding-parameters-angioplasty-balloon-production. Accessed 10 November
31. Chen, Y. (2008). *Modeling and cycle-to-cycle control of the angioplasty balloon forming process*. McGill University (Canada), Canada.
32. Kucklick, T. R. (2012). *The medical device r&d handbook*. Baton Rouge, United States: Taylor & Francis Group.
33. *How products are made: An illustrated guide to product manufacturing* (2001). (Vol. 6, epdf.pub). Farmington Hills, United States: Gale Group.
34. Klein, P. (2009). Fundamentals of plastics thermoforming. *Synthesis Lectures on Materials Engineering, 1*(1), 1–97. https://doi.org/10.2200/S00184ED1V01Y200904MRE001
35. Holman, T., Hoang, N. H., Dunn, R., Schewe, S., Silberg, K., Parsons, D., et al. (2008). Process for forming medical device balloons. In U. S. P. a. T. Office (Ed.), (B29C 49/64 ed., Vol. B2). United States: Boston Scientific Scimed, Inc.
36. McAllister, E. W. (2013). *Pipeline rules of thumb handbook: A manual of quick, accurate solutions to everyday pipeline engineering problems*. Saint Louis, United States: Elsevier Science & Technology.
37. Li, Z., Xu, L. X., Lu, C. L., Liu, G. Z., & Li, X. Y. (2014). Internal structure changes of nylon 12 in balloon forming process. *Applied Mechanics and Materials; Zurich, 528*, 153–161 https://doi.org/10.4028/www.scientific.net/AMM.528.153.
38. Yanes, D., & Mabry, E. (2012). Balloon forming innovations improve quality and reduce cost. *Medical Design Technology, 16*(8), 16–19.
39. Athanasiou, L., Rigas, G., Sakellarios, A., Exarchos, T., Siogkas, P., Bourantas, C., et al. (2016). Three-dimensional reconstruction of coronary arteries and plaque morphology using CT angiography - Comparison and registration with IVUS. *BMC Medical Imaging*. https://doi.org/10.1186/s12880-016-0111-6
40. Lim, F., Owens, T., Sridharan, S., & Le Long, C. (2006). Method of making a low profile balloon. In U. S. P. a. T. Office (Ed.), (B29C 49/22 ed., Vol. US 7,147,817 B1). United States: Abbott Cardiovascular Systems Inc.
41. Laughlin, M. E., Stephens, S. E., Hestekin, J. A., & Jensen, M. O. (2021). Development of custom wall-less cardiovascular flow phantoms with tissue mimicking gel. *Cardiovascular Engineering and Technology*. https://doi.org/10.1007/s13239-021-00546-7
42. BW-TEC AG.(2014, March 27). BW-TEC Balloon moulding machine 503. (0:15 ed.). *Youtube*. Retrieved 2021, November 20, from https://www.youtube.com/watch?v=q1poHbYTghg&t=16s